Bimaterial Proof Mass Capacitive Micro Accelerometer For Increasing Sensitivity

Maryam Sabet Imani[1],

1-Faculty of New Science & Technologies, University of Tehran, Karegar St,Tehran, Iran

Abstract

This paper presents a new approach to improve the performance of MEMS capacitive accelerometer using a metal block in the proof mass structure. In addition, for the design of the capacitive accelerometer is focused on the spring geometry and is shown that the length of long beam and thickness of the serpentine spring are critical parameters which should be optimized to decrease the spring constant in the sense direction and increase it in other directions. The finite element method simulator, ANSYS, is used to find optimum dimensions and to predict specifications of the accelerometer. Sensitivity is increased from 42.853 to 17.7 pF/G and the noise floor is decreased from 52.1 to 21.9 $\mu m/\sqrt{Hz}$ by adding the cupper block in the proof mass. The resonance frequency is dropped from 36955 to 23769 Hz, too.
Keywords: *MEMS accelerometer-capacitive-large proof mass-sensitivity-spring-optimization*

Introduction

MEMS accelerometer provides the advantages of low cost, low power, high precision, high performance, etc. So they are needed in many applications such as aerospace industry, navigation, oil exploration, earth predictions, consumer electronics, etc[1-6]. Capacitive sensing mechanism MEMS accelerometers are popular because they offer high sensitivity, stable DC characteristics, low drift current, low power consumption, and low temperature sensitivity[1].

Some efforts have been taken to improve the performance of MEMS capacitive accelerometer that could be classified in several ways such as reduction of damping coefficient using the vacuum packaging[1], damping holes[2,3], and corrugated electrodes, optimization of the air gap spacing by minimizing both circuit and Brownian noises[2], optimization of flexure geometry[4], d)increasing the inertial mass . The most effective way to improve the performance is increasing the inertial mass which is typically achievable using sillicon-on-insulator(SOI) or wafer-bonded accelerometers[1].   The structure with all silicon wafer thickness and high aspect ratio sense gapes is a way to have a large mass. By this approach they could achieve to the micro gravity accelerometer which had high device sensitivity. However this structure needed double-sided multi-mask process[5]. Novel process named HARPSS which is a single-sided single wafer process that could generate high aspect ratio sense gapes in range of 30-150µm thicknesses. But, this process is complex and

releasing the structure is by wet etching that stiction may occur[2]. An extra seismic mass was added from the backside of the device to increase the proof mass[3]. Selective electroplating of nickel blocks can easily improve the performance because nickel films has larger density and elastic modulus than polysilicon. But this approach just could be applied in CMOS-MEMS accelerometers[6].

However, because of so many applications of MEMS capacitive accelerometers, research on this sensors is continued to have better performance and reduce the cost.

This work reports on a novel structure with biomaterial proof mass and the design optimization of a y-axis capacitive accelerometer.

Structure and operating principle

This accelerometer consists of a proof mass which is suspended by four serpentine springs located each corner of the proof mass. On both sides of mass, there are two sets of fingers known as rotors and fixed fingers are parallel to them known as stators, see fig.1. Each rotor and stator operate as plate of a capacitor known as C_1. A lumped model of the capacitive accelerometer as shown in fig.2 can be reduce to a spring-mass damped model. When an external acceleration is applied to the sensor, the harmonic force function $F = F_0\sin(\omega t)$ drives the mass in the direction of the acceleration. The lumped model can be expressed as a second order differential equation for the displacement y as a function of the external acceleration:

$$m\ddot{y} + B\dot{y} + ky = ma = ma_0\sin(\omega t) \qquad (1)$$

Where m, B, k, and a_0 are the proof mass, damping coefficient, spring constant, and magnitude of the external acceleration applied to the proof mass.

The equation 1 converts to a Laplace transfer function as:

$$H\ s\ = \frac{y\ s}{a\ s} = \frac{1}{s^2+ s\frac{B}{m} + \frac{k}{m}} = \frac{1}{s^2+ s\frac{\omega_0}{Q} + \omega_0{}^2} \qquad (2)$$

Where $\omega_0 = \overline{k/m}$ is the resonance frequency and the quality factor is defined as $Q = \omega_0 m/B$. At the low frequency ($\omega \ll \omega_0$) , the mechanical sensitivity is:

$$\text{mechanical sensitivity} = \frac{y}{a} = \frac{1}{\omega_0{}^2} = \frac{m}{k} \qquad (3)$$

When there is no acceleration, the static capacitance is described as:

$$C_0 = \frac{\varepsilon_0 N l_{eff} t}{g_0} \qquad (4)$$

1. M.S. student, Tel: 09127348995, e-mail: maryam.s.imani@ut.ac.ir

Where l_{eff}, t, N, g_0 are the overlapping length between electrodes, thickness of structure, number of electrodes and air gap, respectively.

When the rotors are moved toward the stators with a displacement Δy, the capacitance can be expressed as:

$$\Delta C = C_1 - C_0 = \frac{\varepsilon A}{g_0 - \Delta y} - \frac{\varepsilon A}{g_0} = \frac{\varepsilon A \Delta y}{g_0(g_0 - \Delta y)} \quad (5)$$

Assume that $\Delta y \ll g_0$:

$$\Delta C \cong \frac{\varepsilon A \Delta y}{g_0^2} = C_0 \frac{\Delta y}{g_0} \quad (6)$$

So the sensitivity can be obtained as[7]:

$$S = \frac{\Delta C}{a} = \frac{C_0}{g_0 \omega_0^2} \quad (7)$$

An important problem is noise. The Total Noise Equivalent Acceleration (TNEA) of a capacitive accelerometer include the Mechanical Noise Equivalent Acceleration and the Electrical Noise Equivalent Acceleration (ENEA) is[2]:

$$TNEA = \overline{MNEA^2 + ENEA^2} = \frac{4k_B TB}{m^2} + \frac{\Delta C_{min}}{S} \quad (8)$$

Where k_B, T, m, B , ΔC_{min}, S are the boltzman constant, absolute temperature, mass of sensor, damping coefficient, circuit minimum resolvable capacitance change, static sensitivity, respectively. The minimum measurable acceleration is limited by TNEA so it should be considered to be minimize.

Spring design
There are many types of flexural spring topologies can be utilized in an accelerometer. As shown in fig.2, the serpentine flexure is used in this work because the small spring constant can be made in a small area and residual stress and extensional axial stress are released through bending of meanders.

According to eq. (3), sensitivity has a inversely relationship with the stiffness. Thus the conventional way to increase the sensitivity is optimization of the spring geometry. In this way, the spring constant of structure should be reduced significantly in the sense direction and be increased in other directions.

In Fedder thesis, the spring constant in all directions for odd meanders was calculated. In order to find the spring constant, only the displacement from bending and torsion is considered and the deformation from shear, beam elongation, and shortening is neglected. Dimensions of serpentine spring is plotted in fig.3. theoretical spring constants are:

$$k_x = [48EI_{z,b}[(3a + b)n - b]]/[a^2 n[(3a^2 \quad (9)$$
$$+ 4ab + b^2)n^3 - 2b(5a + 2b)n^2 + (5b^2$$
$$+ 6ab - 9a^2)n - 2b^2]$$

$$k_y = [48EI_{z,b}[(a + b)n^2 - 3bn + 2b]]/[b^2 \quad (10)$$
$$[(3a^2 + 4ab + b^2)n^3 - 2b(5a + 2b)n^2$$
$$+ (5b^2 + 6ab - 9a^2)n - 2b^2]$$

$$k_z = [48S_{ea}S_{eb}S_{ga}S_{gb}]/[S_{eb}S_{ga}a^2(S_{gb}a + S_{ea} \quad (11)$$
$$b)n^3 - 3S_{ea}S_{eb}S_{ga}a^2 bn^2 + S_{ea}b(2S_{eb}S_{ga}a^2$$
$$+ 3S_{eb}S_{gb}ab + S_{ga}S_{gb}b^2)n - S_{ea}S_{ga}S_{gb}b^3]$$

Where a, b, n, E, G, $and\ l_{z,b}$ are the short beam length, long beam length, number of meanders, elastic modulus, shear modulus, and moment of inertia respectively. Other parameters are $S_{ea} \equiv EI_{x,a}$, $S_{eb} \equiv EI_{x,b}$, $S_{ga} \equiv GJ_a$, $S_{gb} \equiv GJ_b$ where J is the polar moment of inertia[8]
For the design of the spring we have studied effect of the thickness and length of short and long beam on the spring constant which electrostatic forces are neglected.

The spring constant and resonance frequency has been carried out using the static structural and modal tools of ANSYS modulator.

Variation of thickness
The thickness of serpentine spring is varied while the length of short beam and long beam are taken as $20\mu m$ and $100\mu m$, respectively. the Stiffness in directions of x, y, and z with respect to the thickness is plotted in fig.4. k_x and k_y are strongly agreement with theoretical values. In the small thickness, k_z can be verified by eq. (9,10), but, while the thickness is increased, simulation values of k_z show a large error from the theoretical values. As the thickness of sensor increases, the spring constant increasing.

In order to take an optimum thickness, we need another issue. The cross-axis sensitivity defined as the sensitivity in the transverse direction to the lateral sensitivity ratio, which is proportional to $(\frac{f_y}{f_z})^2$. The cross axis sensitivity for different thicknesses is shown in fig.5. As y-direction have been taken for sense direction, cross-axis sensitivity should be less than 1 and very small. Thus $t = 60\mu m$ is a suitable value that could be fabricated by DRIE tools. On the other hand, the large thickness lead to a large mass.

variation of short beam length
The length of the short beam is varied keeping the long beam length and thickness constant at $100\mu m$ and $60\mu m$, respectively. As shown in fig.6, the stiffness is not affected from short beam length strongly. thus $a = 20\mu m$ is taken to fabricate easily.

variation of long beam length
The length of long beam is varied keeping the short beam length at $20\mu m$ and thickness at $60\mu m$. As illustrated by fig.7, k_y decreases as the length of long beam is increased, so larger b is better.

The cross axis sensitivity against the long beam length is plotted in fig.8, so we choose $b = 100\mu m$ to have a small area and small off-axis sensitivity.

parameters in optimum condition
Considering above value, other parameters is taken to have a simple fabrication process and large mass. the geometrical parameters of the proposed accelerometer are listed in Table 1.

Table 1: geometrical parameters of accelerometer

parameter	dimension
proof mass area	$200 \times 400 \ \mu m^2$
cupper block area	$180 \times 380 \ \mu m^2$
overlapped electrodes	$90 \times 60 \ \mu m^2$
air gap	$2 \mu m$
long beam length	$100 \mu m$
short beam length	$20 \mu m$
number of meanders	5
thickness	$60 \mu m$

bimaterial proof mass

In order to increase the displacement of the proof mass for a constant acceleration, increasing the proof mass is a suitable way. As illustrated in eq. (3), the mechanical sensitivity is directly proportional to mass and in eq.(8) MNEA is inversely proportional to it. Thus the large mass lead to the better performance. Middle of the previous proof mass is etched, then is filled by cupper to increase mass of the structure. Cupper is taken because it is denser than polysillicon .

The finite element method simulator, $ANSYS^{TM}$, is used to simulate the mechanical behaviors of such structure. A varied acceleration up to 50G is applied to the structure as shown in fig.9. The displacement and capacitance change are plotted against the acceleration in fig.10 and fig.11, respectively. Von-Mises stress at maximum acceleration is enough small from yield stress of polysillicon .Specifications of bimaterial proof mass accelerometer are listed in Table 2.

Table 2: specifications of bimaterial proof mass ccelerometer

	Without cu block	With cu block
Mass[kg]	1.65×10^{-8}	3.91×10^{-8}
Mechanical sensitivity[m/G]	18.5×10^{-12}	44.8×10^{-12}
Sensitivity[pF/G]	17.7	42.853
Resonance frequency(y)[Hz]	36955	23769
Resonance frequency(x)[Hz]	60351	39.081
Resonance frequency(z)[Hz]	46979	73056
MNEA[$\mu G / \sqrt{Hz}$]	52.1	21.9

The simulation results show the resonance frequency drops from 36955 Hz to 23769 Hz (electrodes are considered in this simulation), so the mechanical sensitivity change from 18.5×10^{-12} to 44.8×10^{-12} m/G after adding the cupper block. MNEA is suppressed 2.3-fold . Thus device performance is improved significantly.

Conclusions

The design optimization of a MEMS comb-drive accelerometer with the serpentine spring has been carried out using analytical and simulation results. The finite element software simulator, ANSYS, was utilized to show relationship between the stiffness and design parameters. An important issue, the cross axis sensitivity, for different long beam lengthes and thicknesses was shown to help us taking optimum values. The long beam length and thickness was illustrated are effective parameters and increase them

lead to better performance, but overall device area limited it. A novel structure, bimaterial proof mass, was taken to improve the sensitivity and noise floor. The cupper block in middle of the proof mass lead to mass larger from 1.65×10^{-8} to 3.919×10^{-8} kg . Simulation results show the mechanical sensitivity was increased 2.4-fold and noise floor is decreased 2.3-fold. Thus this structure seems have better performance by adding cupper block.
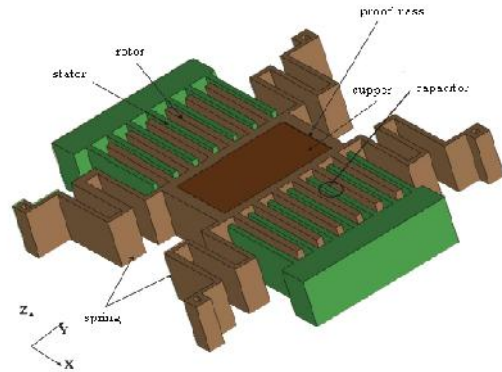

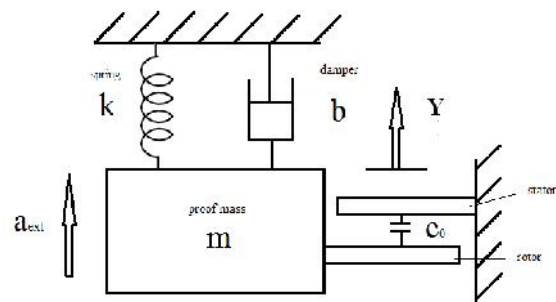Fig. 1: Schematic of bimaterial proof mass capacitive micro accelerometer.

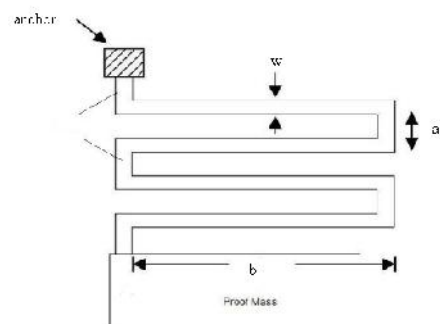Fig. 2: Lumped model of the capacitive accelerometer
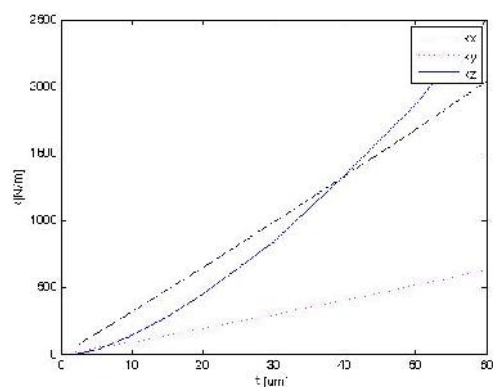.

Fig. 3: Serpentine spring parameters.

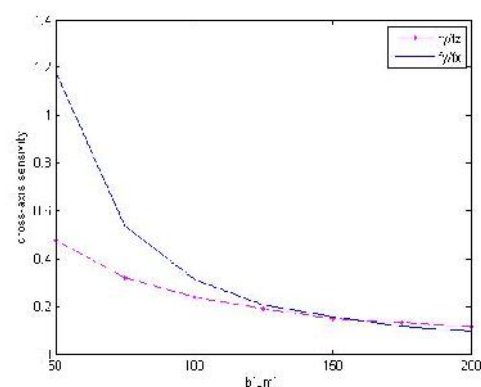Fig. 4: The spring constant with respect to the thickness.

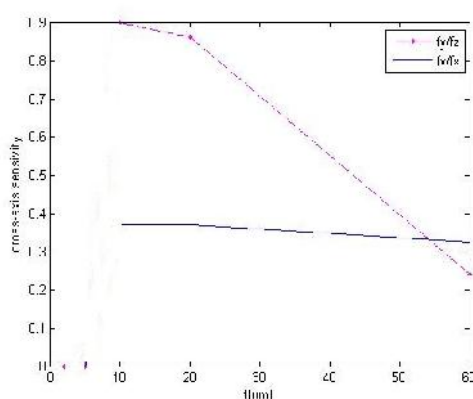Fig. 8: The cross-axis sensitivity Vs the long beam thickness.

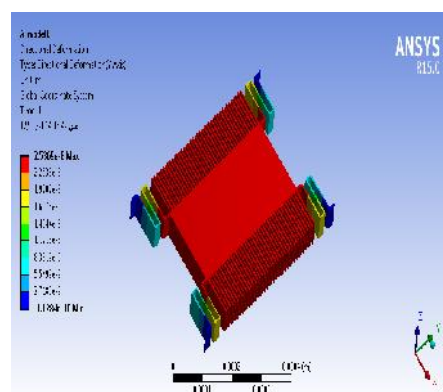
Fig. 5: The cross-axis sensitivity Vs the thickness.

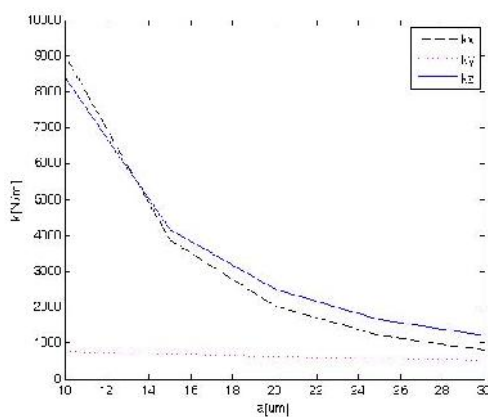
Fig. 9:The acceleration applied to the structure.

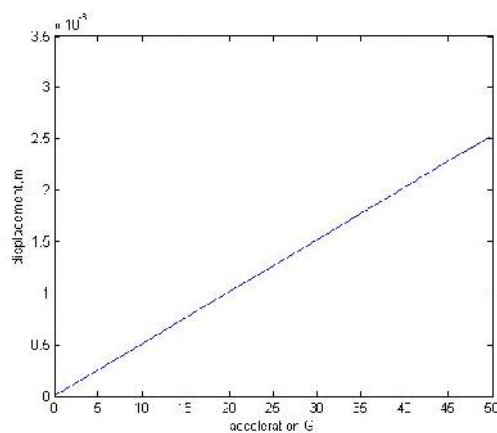Fig. 6: The spring constant with respect to the short beam length.
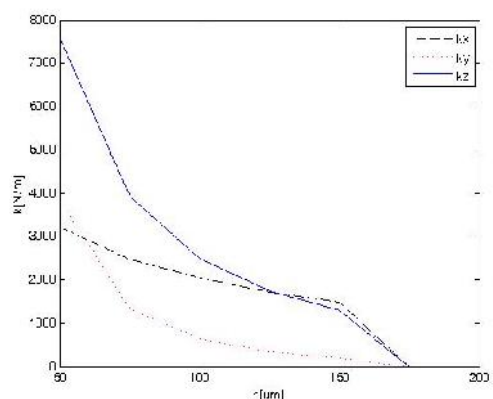

Fig. 10: The isplacement against acceleration.

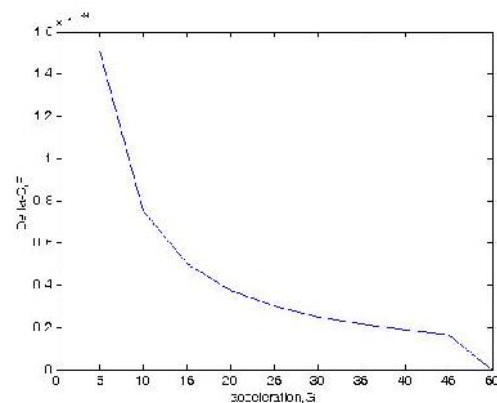Fig. 7: The spring constant with respect to the long beam length.

Fig. 11: The capacitance change against acceleration.

References

1- Chae J., Kulah H. and Najafi Kh., An In-plane High-Sensitivity, Low-Noise Micro-g Sillicon Accelerometer With CMOS Readout Circuitry, *Journal Of Microelectromechanical Systems*, Vol. 13, No. 4, 2004, pp. 628-635.

2- Monajemi P and Ayazi F., Design Optimization and Implementation of a Microgravity Capacitive HARPSS Accelerometer, *IEEE Sensors Journal*, Vol. 6, No. 1, 2006, pp. 39-46.

3- Abdolvand R., Vakili Amini B. and Ayazi F., Sub-Micro-Gravity In-Plane Accelerometers With Reduced Capacitive Gaps and Extra Seismic Mass, *Journal Of Microelectromechanical Systems*, Vol. 16, No. 5, 2007, pp. 1036-1043.

4- Pant B.D., Dhakar L., George P.J. and Ahmad S.,Design of a MEMS Capacitive Comb-drive Micro-accelerometer with Sag Optimization, *Sensors & Transducers Journal*, Vol. 108, No. 9, 2009, pp. 15-30.

5- Yazdi N. and Najafi Kh., An All-Silicon Single-Wafer Micro-g Accelerometer with a Combined Surface and Bulk Micromachining Process**,** *Journal Of Microelectromechanical Systems*, Vol. 9, No. 4, 2000, pp. 544-550.

6- Liu Y.C., Tsai M.H., Tang T.L. and Fang W., Post-CMOS selective electroplating technique for the improvement of CMOS-MEMS accelerometers, *Journal Of Micromechanics And Microengineering*. Vol. 21, 2011.

7- Chen J.Y., *single and dual-axis lateral capacitive accelerometers based on CMOS-MEMS technology*, master thesis, University of Oslo 2010.

8- Fedder G.K., *Simulation of Microelectromechanical Systems*, PhD thesis, University of California, 1994.